

MAGNETIC ANALYSIS OF TWO [COBALT- IMIDAZOLE-CARBOXYLATE] COMPLEXES: ORBITAL CONTRIBUTION

RAMON ARRUE,^{1,2} DOMINIQUE TOLEDO,¹ OCTAVIO PEÑA,³ JEAN-YVES PIVAN,^{3,4} MARIO REIS,⁵ YANKO MORENO*⁶

¹Universidad de Concepción, Facultad de Ciencias Químicas, Departamento de Química Analítica e Inorgánica, Concepción, Chile

²Universidad Santo Tomás, Departamento de Ciencias Básicas, Concepción, Chile

³Institut des Sciences Chimiques de Rennes, UMR 6226, Université de Rennes-1, Rennes, France

⁴École Nationale Supérieure de Chimie de Rennes, Rennes, France

⁵Instituto de Física, Universidade Federal Fluminense - Av. Gal. Milton Tavares de Souza s/n, 24210-346, Niterói, Rio de Janeiro, Brazil

⁶Universidad Andrés Bello, Departamento de Cs. Químicas, Facultad de Cs. Exactas, PC 2520000, Viña del Mar, Chile

ABSTRACT

Two coordination complexes, $\text{Co}(\text{HIMC})_2(\text{H}_2\text{O})_2$ (**1**) and $\text{Co}(\text{H}_2\text{IMDC})_2(\text{H}_2\text{O})_2$ (**2**), were synthesized by mixing the complex precursor Cobalt(II) hexafluoroacetylacetonate ($\text{Co}(\text{hfacac})_2$) with 1H-imidazole-4-carboxylic acid (H_2IMC) and 1H-imidazole-4,5-imidazoledicarboxylic acid (H_3IMDC) ligands.

These compounds have been isolated as neutral, air and thermal stable solid and have been characterized by FT-IR and powder X-Ray diffraction analysis. The thermal stability and magnetic properties were studied in the solid state.

Compounds (**1**) and (**2**) are mononuclear complexes, where the cobalt ions adopt an distorted octahedral geometry. At low temperature they exhibit a weak antiferromagnetic interaction. The contribution of the angular momentum to the magnetic moment as well as intermolecular interactions were taken into consideration for the quantitative modeling of their magnetic properties

1. INTRODUCTION

The synthesis and design of Metal Organic Frameworks (MOF) based on multidentate ligands such as polycarboxylate and N-heterocyclic ligands, have brought significant interest owing to their fascinating architectures and useful properties such as magnetism,^{1,2} porosity,³⁻⁵ luminescence,^{6,8} etc.

It is well-known that aromatic polycarboxylates, especially the N-heterocyclic carboxylates, are excellent building blocks due to their versatile coordination modes and potential hydrogen bonding capabilities, giving additional opportunities to obtain diverse metal-organic assemblies, that includes multidimensional coordination polymers as well as discrete supramolecular structures.^{8,9}

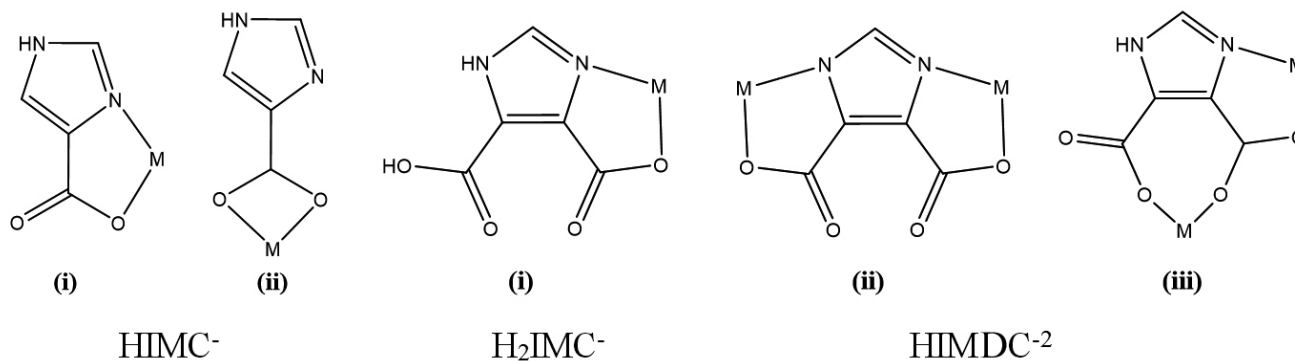
In the search of stable systems with paramagnetic metal centers, the 1H-imidazole-4-carboxylic acid (H_2IMC) and 1H-imidazole-4,5-imidazoledicarboxylic acid (H_3IMDC) have attracted our interest. They are rigid bridging and bifunctional ligands that can be successively deprotonated to generate various species with different proton numbers,^{3,9} such as: HIMC^- and $\text{H}_2\text{IMC}/\text{HIMC}^{2-}$ anions, for H_2IMC and H_3IMC , respectively and can give place to a wide variety of coordination modes,^{10, 11} (Scheme 1). Therefore, these ligands have great potential for coordinative interactions and hydrogen

bonding, allowing the interaction among paramagnetic centers with the opportunity to observe magnetic coupling.

Taking this into consideration, herein we report the successful attempts for the synthesis, structural exploration of two Co(II) complexes with discrete structures, formed by the reaction of H_2IMC and H_3IMDC ligands and Co(II) hexafluoroacetylacetonate [$\text{Co}(\text{hfacac})_2$], the final products being formulated as $\text{Co}(\text{HIMC})_2(\text{H}_2\text{O})_2$ (**1**) and $\text{Co}(\text{H}_2\text{IMDC})_2(\text{H}_2\text{O})_2$ (**2**).

Due to the poor solubility and the paramagnetic nature of **1** and **2**, they have been characterized by thermogravimetric analysis and powder X-ray diffraction. The structural analysis reveals that the hfacac groups do not take part in the final product, being volatilized during the synthesis process.

Moreover, the magnetic properties of **1** and **2** were studied by thermal and field dependent magnetic susceptibility measurement. For both compounds, the magnetic data show deviations to the Curie law at low temperatures, that indicate a magnetic cooperation phenomenon between the paramagnetic centers. The chemical structure and magnetic experimental data were analyzed and modeled considering the spin-orbit coupling present in semi-octahedral Co(II) compounds with a high-spin electronic state. This could be important since this contribution is essential to design single molecule magnets (SMM).



Scheme 1. Possible coordination modes for HIMC^- , H_2IMC^- and HIMDC^{2-} anions.

2. EXPERIMENTAL

All chemicals purchased were of reagent grade or better and used without further purification.

2.1 Syntheses of Complexes.

• $\text{Co}(\text{HIMC})_2(\text{H}_2\text{O})_2$ (**1**)

0.1489 g of H_2IMC (1.33 mmol) was dissolved in 12.75 mL NaOH dissolution (0.199 mol L^{-1}). 0.3221 g of $\text{Co}(\text{hfacac})_2$ (0.681 mmol) were dissolved in 10 mL absolute ethanol. The dissolutions were stirred and after 2 hr. an orange solid was formed and filtered in vacuum using a porous glass filter obtaining a pale orange solid. This product was washed with 10 mL cool deionized water and 15 mL absolute ethanol and then dried overnight at 70°C. Yield: 183 mg (0.577 mmol, 85%). IR (KBr pellets, cm^{-1}) 3144vs, 1694m, 1553vs, 1463m, 1401vs, 1230m, 1096m, 1007m, 928w, 835m, 791m, 658m.

• $\text{Co}(\text{H}_2\text{IMDC})_2(\text{H}_2\text{O})_2$ (**2**)

H_2IMDC ligand (0.1500 g, 0.961 mmol) was dissolved in a baker with 30 mL of deionized water and 3.45 mL of NaOH dissolution (0.276 mol L^{-1}) and left stirring in a round bottom flask. Then, when all the ligand was dissolved, 0.4548 g of $\text{Co}(\text{hfacac})_2$ (0.952 mmol) previously dissolved in 10 mL of absolute ethanol was added. A pale orange suspension was formed which was left stirring for 3 hours and filtered under vacuum using a porous glass filter. The solid was washed first with 10 mL cool water and 15 mL of cool ethanol and then dried overnight at 70°C. Yield: 182 mg (0.449 mmol, 47%). IR (KBr pellets, cm^{-1}): 3316vs, 3226vs, 1744m, 1500vs, 1243m, 1009m, 786m, 648m, 521w, 450s.

2.2 Spectroscopic and photophysical measurements.

Infrared spectra. Infrared spectra were obtained from KBr pellets on a Perkin-Elmer 1600 FT-IR spectrophotometer in the range from 4000 to 400 cm^{-1} . Dried product was pulverized and mixed in 1%wt with spectroscopic grade KBr and molded in the shape of thin discs in a hydraulic press.

Thermogravimetric analysis. Thermogravimetric analysis were performed using a TA Instruments model SDT Q600 with heating program from 20°C to 700°C. A polycrystalline sample was dried overnight in an oven at 100°C and then about 6 mg sample was placed in a platinum sampleholder inside the instrument. Depending on the nature of the experiment, the measurement was performed in an inert N_2 atmosphere or in an oxidant synthetic air atmosphere, in both cases under a 50 mL min^{-1} gas flow.

X-ray powder diffraction measurements were carried out at ambient temperature in a Bruker D8 Discovery diffractometer with $\text{Cu-K}\alpha 1$ radiation ($\lambda = 1.5406\text{\AA}$), Ge(111) monochromator and a surface CCD detector. The Bragg positions were extracted by pattern decomposition and then indexed to obtain the cell parameters using the software suite *FullProf*.¹² The diffraction data were taken from 5.00° to 80.00° (2 θ) with a stepsize of 0.02° and steptime

of 300 ms.

Magnetic measurements The Magnetic susceptibility measurements were carried out with powdered samples using a SQUID magnetometer (Quantum Design MPMS-XL5) at constant field (0.5 kOe) from 2 K to 300 K, and at constant temperature (2 K) from 0 to 10 kOe. The diamagnetism from the sampleholder was corrected and the diamagnetic contribution estimated from Pascal tables. About 100 mg of polycrystalline sample were placed under a magnetic external field of 500 Oe and the magnetic response was measured as a function of the temperature warming from 2 K to 300 K.

3. RESULTS AND DISCUSSION

3.1 Synthesis and characterization of cobalt(II) complexes

Compounds **1** and **2** were separated as air-stable solids in good yields and were characterized by infrared spectroscopy, X-ray diffraction in powdered samples, thermogravimetric analyses and magnetic measurements.

The choice of the organic ligands as well as the metal salts and the addition of the NaOH in an appropriate proportion was essential to the final result. It is important to note that, although different methods of synthesis were tested to crystallize these compounds, due to the low solubility of **1** and **2** in common solvents, all attempts to get crystals of good quality were unsuccessful. However, compounds **1** and **2** were fully studied by powder X-Ray diffraction.

The FT-IR spectra of compounds **1** and **2** exhibit strong and broad absorption bands in the range of 3600-3300 cm^{-1} due to the presence of $\nu(\text{O-H})$ and $\nu(\text{N-H})$ stretching vibration mode of the coordinated water molecules and the imidazole ring respectively.

Additionally, for compound **1** the absence of any strong band around 1700 cm^{-1} indicates that the acid function in the H_2IMC ligand is deprotonated, while the $\nu(\text{C=O})$ absorption band of compound **2** at 1740 cm^{-1} indicates that one carboxyl group of the ligand remains protonated. A series of bands between 1600-1300 cm^{-1} indicates the presence of the $\nu(\text{C=O})$, $\nu(\text{C=C})$ and $\nu(\text{C=N})$ bonds. These IR spectra are in good agreement with the powder X-ray structural characterizations.

3.2 Thermogravimetric analysis.

In order to check examine the thermal stability of compounds **1** and **2**, thermal gravimetric measurements were carried out in a N_2 atmosphere in the temperature range between 20 and 800 °C. **Fig. 1** shows the TG and DTG curves for **1** and **2**.

Through this experiment it was found that the hfacac groups do not take part in the synthesized compounds. Considering the hypothetical presence of two imidazole carboxylic ligands, two hfacac diketones molecules and one cobalt metal center by one molecular entity, the analysis on the decomposition profile revealed that a different products were obtained.

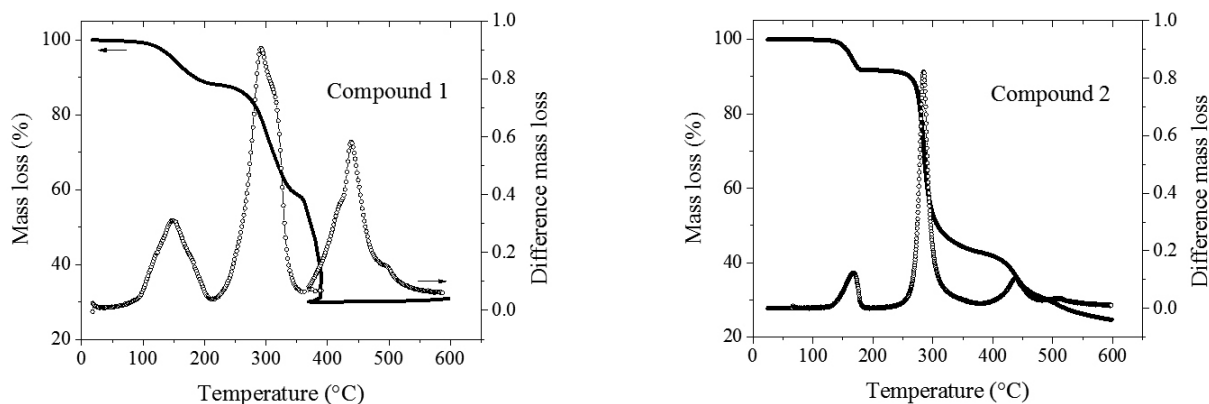


Fig 1. Thermogravimetric Analysis (TGA, solid line) and Derivative Thermogravimetry (DTG, circles) profiles for compounds (**1**) and (**2**) in N_2 atmosphere.

In a first approximation, it was expected a first decomposition step attributed to the volatilization of the hfacac groups. In these molecules, the presence of electron-withdrawing $-\text{CF}_3$ groups can make the M-hfacac bond weaker and, as a consequence, it should be liberated at a lower temperature.

However, for compound **1** a first weight-loss process occurs from the

beginning of the experiment up to 220°C, indicating the volatilization of 12% of the total mass. This mass change along with the observed temperature range suggests that there are no hfacac molecules coordinated to the cobalt atom. Subsequent to this, the second decomposition process takes place at 370°C with a mass loss of 33%.

Reviewing a previous work published by Premkumar et. al.¹³ describing thermogravimetric analysis of several coordination compounds based on imidazole carboxylic ligands, it was founded that carboxylic groups are decomposed around this temperature. Above this temperature, the rest of the organic residue is decomposed in nitrogen inert atmosphere.

Taking into account the possibility of coordinated water molecules instead of hfacac ligands, the analysis of the decomposition steps based on the mass loss percentage is in agreement with a $\text{Co}(\text{HIMC})_2(\text{H}_2\text{O})_2$ formula (molar mass=317.13 g mol^{-1}).

In the same way, for compound 2 three weight-loss processes were observed. The first weight-loss of 8.2% takes place between 120°C to 185°C, suggesting that there are no hfacac molecules coordinated to cobalt atom, so this loss is attributed to the release of coordinated water molecules. After that, in the range 225–380 °C the structure starts to collapse, with a single-step weight loss of 53%. The product obtained is relatively unstable and decomposes between 380–485°C, showing a mass loss of ~29%. Above this temperature, the decomposition continues until our limiting temperature of 600 °C. Taking into consideration this scenario, the formula $\text{Co}(\text{H}_2\text{IMDC})_2(\text{H}_2\text{O})_2$ can satisfactorily explain the decomposition profile.

All these hypotheses about the structure of the synthesized compounds were confirmed by powder X-ray diffraction.

3.3 X-ray powder diffraction analyses.

Due to the poor solubility of compounds 1 and 2 in many solvents, structural characterization was performed by powder X-ray diffraction.

Considering the evidence obtained in the thermogravimetric analysis, X-ray powder diffraction patterns were studied under the idea of a $\text{Co}(\text{L})_2(\text{H}_2\text{O})_2$ formula, where L is an imidazole carboxylate ligand.

It was founded that the possible structures for compounds 1 and 2 were previously reported. Therefore, the experimental diffractograms of both compounds were compared with those obtained by simulation from the single crystal data published previously^{7, 14} (Fig 2). The coincidence in the position of the diffraction peaks helps to consider that compounds 1 and 2 correspond to $\text{Co}(\text{HIMC})_2(\text{H}_2\text{O})_2$ and $\text{Co}(\text{H}_2\text{IMDC})_2(\text{H}_2\text{O})_2$ respectively. From this, the structure-property analysis is discussed here below considering the crystallographic information previously reported.

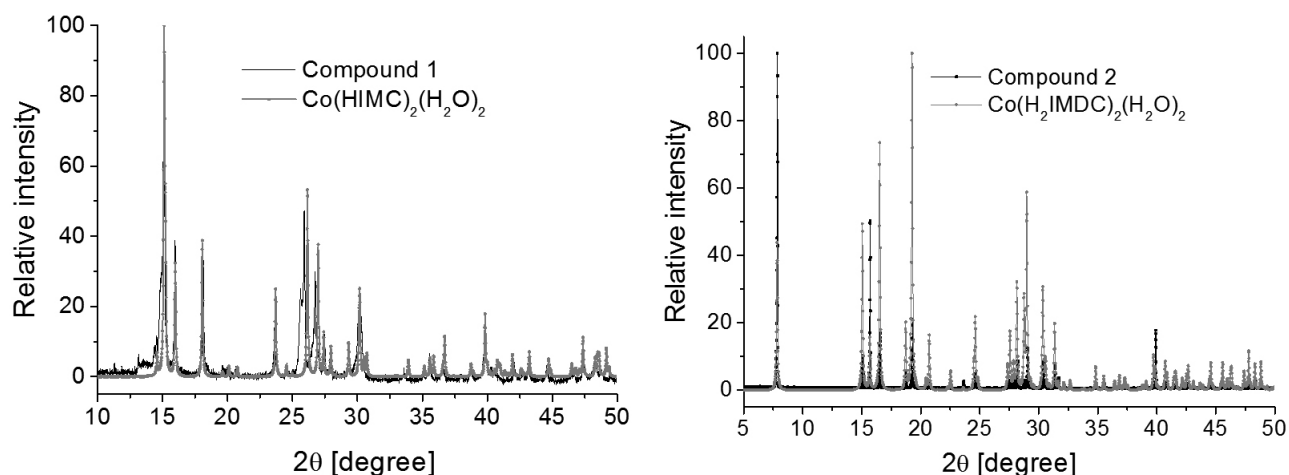


Fig 2. Experimental and computer-simulated XRPD patterns for compound 1 and compound 2.

Compound 1 corresponds to $\text{Co}(\text{HIMC})_2(\text{H}_2\text{O})_2$, where the cobalt appears in a highly distorted octahedral environment surrounded by two imidazole carboxylate ligands in equatorial position and *cis* configuration bonded to the metal by one nitrogen in the imidazole ring and one oxygen atom from the carboxylate group, and two water molecules in axial positions. In Fig. 3 it can be observed the presence of three different intermolecular hydrogen bond interactions. The first H-bond occurs between one hydrogen atom from the coordinated water molecule and the free oxygen atom in the carboxylate group with a D-A (donor-acceptor) distance of 2.81 Å. The second interaction occurs between the hydrogen bonded to the nitrogen atom of the imidazole ring and

the same free oxygen atom in the carboxylate group with a D-A distance of 2.77 Å. The third H-bond arises from the interaction in the opposite direction between the other hydrogen atom in the water molecule and the free oxygen in the carboxylate group in the neighboring molecule with a D-A distance of 2.76 Å. Additionally, two π -interactions are present in the crystal packing between the imidazole ring conjugated system whose distances among centroids (3.58 Å and 5.26 Å) contribute to stabilize the crystal packing. The metal heteroatom bond distances are the following: axial Co-O 2.11 Å, equatorial Co-O 2.18 Å and Co-N are 2.08 Å.

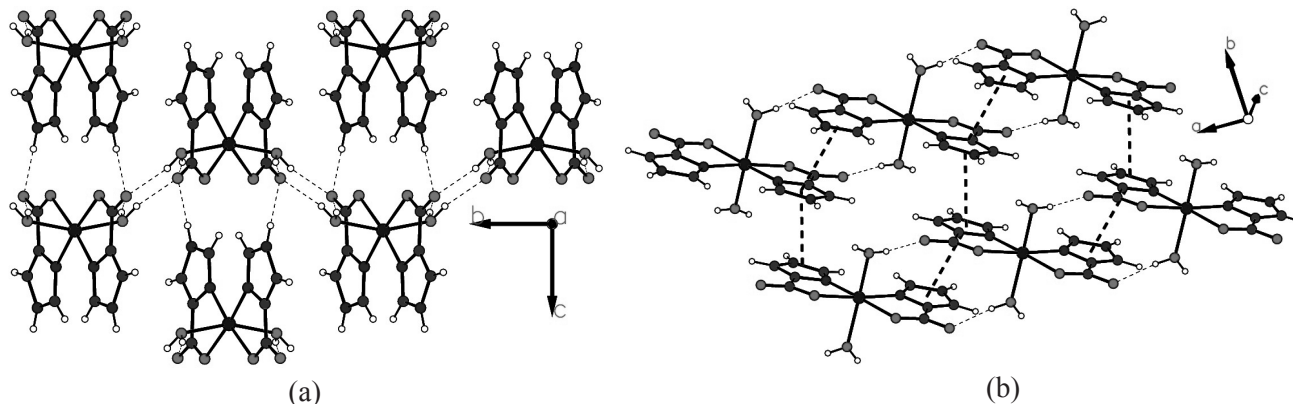


Fig 3. (a) Hydrogen bonds viewed along [100] directions and (b) π - π interactions for compound $\text{Co}(\text{HIMC})_2(\text{H}_2\text{O})_2$ (1).

For compound **2**, the cobalt metal center is coordinated in equatorial position and in *trans* configuration by two imidazole dicarboxylate ligands bonded to the metal center by the nitrogen atom from the imidazole ring and the oxygen atom of one of the carboxylate groups. Two coordinated water molecules in axial positions complete a distorted octahedral geometry. Two different hydrogen bonds were observed (Fig.4), the first between the hydrogen

atom of a water molecule and the free oxygen atom in the coordinating carboxylate group with a D-A distance of 2.49 Å. The second arises from the hydrogen atom bonded to the nitrogen in the imidazole ring and on the oxygen atom in the non-coordinating carboxylate group with a D-A distance of 2.72 Å. The four Co-O bond distances are the same with a value of 2.13 Å, while the Co-N distances are 2.09 Å.

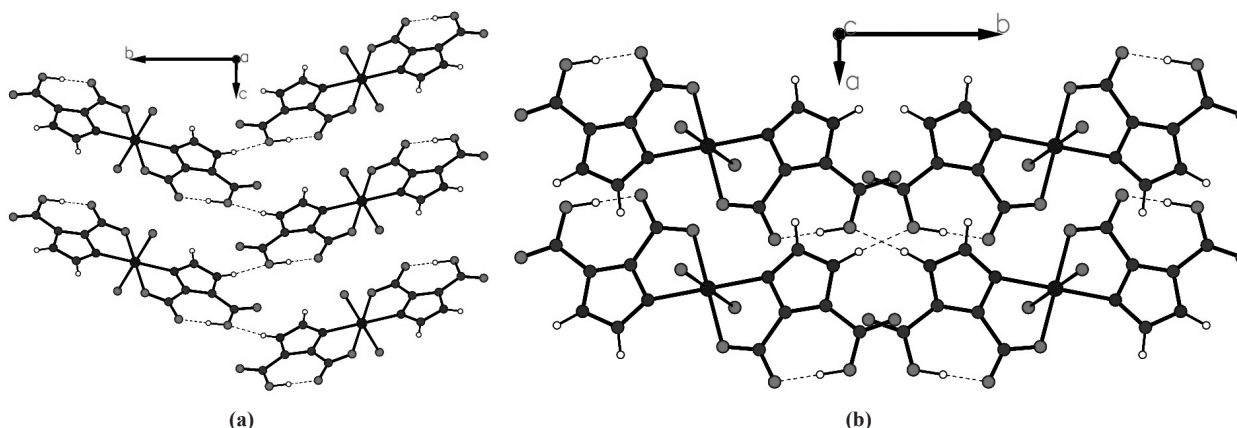


Fig 4: Hydrogen bonds in compound $\text{Co}(\text{H}_2\text{IMC})_2(\text{H}_2\text{O})_2$ (**2**). View along (a) [100] and (b) [001] directions.

The analysis on metal-heteroatom distances anticipates that both complexes are in high-spin electronic state, because the distortions produced by a Jahn-Teller effect for low-spin d^7 ions were not observed. This hypothesis was confirmed by the magnetic susceptibility measurements.

3.4 Magnetic properties

Fig. 5 shows the temperature dependence of $\chi_M \cdot T$ (where χ_M is the molar susceptibility per Co (II) ion) for both compounds **1** and **2**. A slow decrease of $\chi_M \cdot T$ is observed down 50 and 5K respectively, which is relatively common

in compounds with a ground state ${}^4T_{1g}$ (octahedral d^7); these systems undergo spin-orbit coupling (see scheme 2). It is known that those molecules, in which there is an orbital contribution in the ground term (T), exhibit moments larger than those expected for an only spin contribution and that their magnetic moments vary with temperature (while the ground terms A and E give rise to moments independent of temperature and without orbital contribution).¹⁵

At lower temperatures (below 50 and 5 K, for compounds (1) and (2) respectively) a rapid decrease of $\chi_M \cdot T$ below these temperatures, which suggests the possibility of antiferromagnetic coupling (*vide infra*)

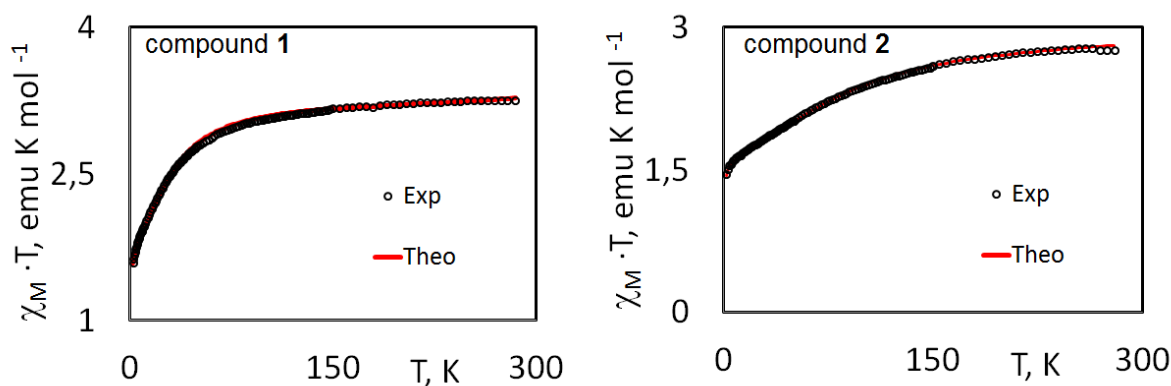
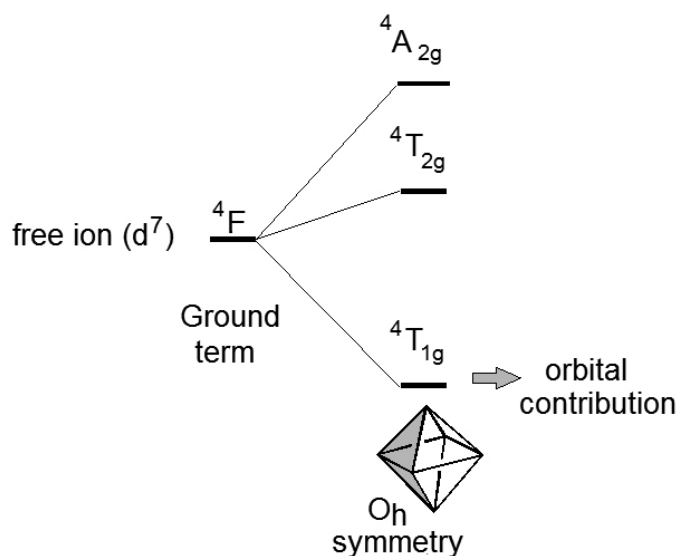


Fig 5: Temperature dependence of $\chi_M \cdot T$ (where χ_M is the molar susceptibility per Co(II) ion) for compounds **1** and **2**. A weak antiferromagnetic interaction is observed for both cases at low temperature.

From the high temperature data analysis (χ_M^{-1} vs T, see Fig. 6) it is deduced a Curie-Weiss behavior for both compounds and it were calculated their magnetic moments: $\mu_1 = 5.0$ [BM] and $\mu_2 = 5.0$ [BM] for compounds **1** and **2**, respectively (these magnetic moments are larger than the spin-only value

of 3.87 [BM], due to the orbital contribution). On the other hand, the Curie constant for compound **1** is $C_1 = 3.12 \text{ cm}^3\text{mol}^{-1}\text{K}$ and for compound **2** is $C_2 = 3.10 \text{ cm}^3\text{mol}^{-1}\text{K}$, leading to g values of $g_1 = 2.58$ and $g_2 = 2.57$, respectively (*vide infra*).



Scheme 2: Under an octahedral field, cobalt (system d⁷, term ⁴F) the ground term ⁴F splits into three states. The ground state is ⁴T_{1g} and an orbital contribution is expected.

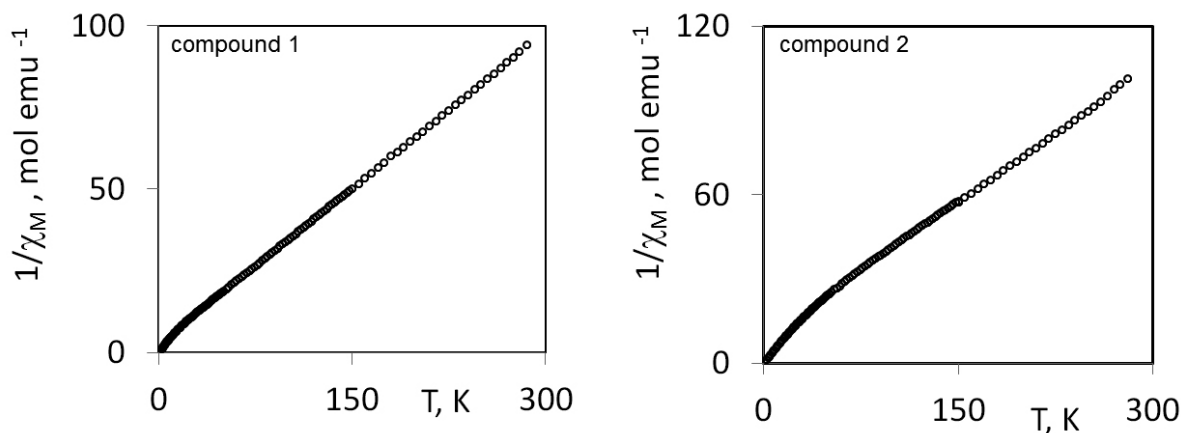


Fig 6. χ_M^{-1} vs T for compound 1 (left) and 2 (right). Curie constants of $C_1 = 3.12$ and $C_2 = 3.10 \text{ cm}^3\text{mol}^{-1}\text{K}$ were observed for (1) and (2) respectively.

Considering a total quenched orbital contribution (that is $L=0$, therefore $J=S$), the magnetic susceptibility can be written as (Eq. 1)¹⁵:

$$\chi_M = \frac{Ng^2\beta^2}{3kT} \cdot J(J+1) \quad (\text{Eq. 1})$$

From the slope of the graph χ_M^{-1} vs T (Fig.6), Curie constants were deduced for compounds 1 and 2; which leads to $C_1 = 3.12$ and $C_2 = 3.10 \text{ cm}^3\text{mol}^{-1}\text{K}$.

Taking $J = 3/2$, $g_1 = 2.58$ and $g_2 = 2.57$ for compounds 1 and 2 respectively.

These high values are due to orbital contribution, which is characteristic of ⁴T_{1g} ground state, belonging to O_h symmetry. Must be considered that an eventual decreased on symmetry (e.g. from O_h to D_{4h}) would imply an A or E ground state, where there would be an orbital quenching (therefore a $g \sim 2$ would be expected).¹⁶

Can be discussed the magnetic data by considering a spin-orbit coupling parameter λ ($H = -\lambda LS$) in a molecular-field approximation.¹⁷ The magnetic susceptibility for mononuclear Co(II), χ_{mono} , in an octahedral environment can be calculated from Eq. 2¹⁶:

$$\chi_{\text{mono}} = \frac{1}{T} \left[\frac{7(3-A)^2 x}{5} + \frac{12(2+A)^2}{25A} + \left(\frac{2(11-2A)^2 x}{45} + \frac{176(2+A)^2}{675A} \right) x \exp\left(\frac{-5Ax}{2}\right) + \left(\frac{(5+A)^2 x}{9} - \frac{20(2+A)^2}{27A} \right) \exp(-4Ax) \right] \left\{ \frac{8x}{3} \left[3 + 2 \exp\left(\frac{-5Ax}{2}\right) + \exp(-4Ax) \right] \right\} \quad (\text{Eq. 2})$$

where $x = \lambda/k_B T$ and A is related with the crystal field strength relative to the interelectronic repulsions¹⁷. The best fitting for compound **1** of $\chi_M \cdot T$ vs T , in the temperature range of 5 to 285 K, gives $\lambda = -53.3 \text{ cm}^{-1}$, $A = 1.3$, with $R = 7.4 \cdot 10^{-5}$ ($R = \Sigma(\chi_{M, \text{obs}} - \chi_{M, \text{calc}})^2 / \Sigma(\chi_{M, \text{obs}})^2$). For compound **2**, in the same temperature range, gives $\lambda = -186.0 \text{ cm}^{-1}$, $A = 1.14$, with $R = 6.9 \cdot 10^{-7}$.

The model reasonably work at the lowest temperatures, when a weak intermolecular interaction was considered. Then, a good fit total adjustment, from 2 to 285K is achieved with Eq. 3,¹⁸ that considers a weak antiferromagnetic interaction between Co(II) centers, with zJ as the total exchange coupling between them:

$$\chi = \frac{\chi_{\text{mono}}}{1 - (2zJ/Ng^2\beta^2)\chi_{\text{mono}}} \quad (\text{Eq. 3})$$

where N , g , β have the usual meanings. The best fitting of the susceptibility data in the temperature range of 2 to 285 K gives for compound **1**, $g = 2.58$, $zJ = -0.175 \text{ cm}^{-1}$, and for compound **2**, $g = 2.57$, $zJ = -0.20 \text{ cm}^{-1}$.

Finally, as discussed before, since these compounds have distorted octahedral geometry, the ground level (${}^4T_{1g}$) could be splitted and generate states in which the orbital contribution is quenched. This situation was analyzed and calculations were performed, but it was not possible up to now to fit a model with physically sustainable theoretical data.

CONCLUSION

Two cobalt- imidazole-carboxylate complexes have been synthesized, $\text{Co}(\text{HIMC})_2(\text{H}_2\text{O})_2$ (**1**) and $\text{Co}(\text{H}_2\text{IMDC})_2(\text{H}_2\text{O})_2$ (**2**); their structures were characterized by thermogravimetric and powder X-ray techniques. The molecular structure reveals that the environment of the cobalt atoms is a distorted octahedral geometry. Their magnetic behavior are in agreement with the existence of an orbital contribution; neglecting the geometric distortion, it is possible to use a theoretical model which explains the orbital contribution to the magnetic moment. For both compounds weak antiferromagnetic interactions were observed at low temperature. With $g = 2.58$, $zJ = -0.15 \text{ cm}^{-1}$, $\lambda = -53.3 \text{ cm}^{-1}$, $A = 1.30$ for compound **1** and $g = 2.57$, $zJ = -0.20 \text{ cm}^{-1}$, $\lambda = -186.0 \text{ cm}^{-1}$, $A = 1.14$ for compound **2**.

ACKNOWLEDGMENTS

This research has been performed as part of the Chilean-French International Associated Laboratory for "Multifunctional Molecules and Materials" (LIA-M3-CNRS N°1027). Financial supports from the Fondo Nacional de Desarrollo Científico y Tecnológico [FONDECYT (Chile), N°1130433], the CNRS and the Université de Rennes 1 are gratefully acknowledged. D. Toledo thanks to CONICYT (Chile) for support of the graduate fellowship N°21120148. Y. Moreno thanks to UNAB DI-773-15/R.

REFERENCES

1. D. Toledo, A. Vega, N. Pizarro, R. Baggio, O. Peña, T. Roisnel, J.-Y. Pivan and Y. Moreno, *Journal of Solid State Chemistry*, 2017, **253**, 78-88.
2. D. Toledo, G. Ahumada, C. Manzur, T. Roisnel, O. Peña, J.-R. Hamon, J.-Y. Pivan and Y. Moreno, *Journal of Molecular Structure*, 2017, **1146**, 213-221.
3. X. Li, B.-L. Wu, C.-Y. Niu, Y.-Y. Niu and H.-Y. Zhang, *Crystal Growth & Design*, 2009, **9**, 3423-3431.
4. P. Liang, W.-X. Xia, W.-M. Tian and X.-H. Yin, *Molecules*, 2013, **18**, 14826-14839.
5. H. Jia, M. Guo, B. Ma, Y. Liu and G. Li, *Synthesis and Reactivity in Inorganic, Metal-Organic, and Nano-Metal Chemistry*, 2013, **43**, 1458-1464.
6. L. Zhao, Z. Wang, D. Zhao and X. Meng, *Synthesis and Reactivity in Inorganic, Metal-Organic, and Nano-Metal Chemistry*, 2014, **44**, 195-202.
7. E. Shimizu, M. Kondo, Y. Fuwa, R. P. Sarker, M. Miyazawa, M. Ueno, T. Naito, K. Maeda and F. Uchida, *Inorganic Chemistry Communications*, 2004, **7**, 1191-1194.
8. Z. Xiong, H. Jia, B. Ma and G. Li, *Synthesis and Reactivity in Inorganic, Metal-Organic, and Nano-Metal Chemistry*, 2012, **42**, 1204-1210.
9. Z.-G. Gu, Y.-T. Liu, X.-J. Hong, Q.-G. Zhan, Z.-P. Zheng, S.-R. Zheng,

- W.-S. Li, S.-J. Hu and Y.-P. Cai, *Crystal Growth & Design*, 2012, **12**, 2178-2186.
10. Q.-G. Zhai, R.-R. Zeng, S.-N. Li, Y.-C. Jiang and M.-C. Hu, *CrystEngComm*, 2013, **15**, 965-976.
11. S. Wang, L. Zhang, G. Li, Q. Huo and Y. Liu, *CrystEngComm*, 2008, **10**, 1662-1666.
12. J. Rodríguez-Carvajal, *Physica B: Condensed Matter*, 1993, **192**, 55-69.
13. T. Premkumar, S. Govindarajan, W. P. Pan and R. Xie, *Journal of Thermal Analysis and Calorimetry* 2013, **35**, 325-333.
14. B. Artetxe, L. San Felices, A. Pache, S. Reinoso and J. M. Gutiérrez-Zorrilla, *Acta Crystallogr. Sect. E Struct. Reports Online* 2013, **69**, 94.
15. A. Earnshaw, *Introduction to Magnetochemistry*, Academic Press INC. (London) LTD, Berkeley Square, London W.1, 1968.
16. F. Lloret, M. Julve, J. Cano, R. Ruiz-García and E. Pardo, *Inorganica Chimica Acta*, 2008, **361**, 3432-3445.
17. H.-L. Sun, Z.-M. Wang and S. Gao, *Inorganic Chemistry*, 2005, **44**, 2169-2176.
18. O.Kahn, *Molecular Magnetism*, Wiley-VCH, New York, 1993.